# Journal of Vertebrate Paleontology

# Osteology of the large dissorophid temnospondyl *Anakamacops petrolicus* from the Guadalupian Dashankou Fauna of China

## Jun Liu

ARTICLE

# OSTEOLOGY OF THE LARGE DISSOROPHID TEMNOSPONDYL *ANAKAMACOPS PETROLICUS* FROM THE GUADALUPIAN DASHANKOU FAUNA OF CHINA

JUN LIU

Key Laboratory of Vertebrate Evolution and Human Origins of Chinese Academy of Sciences, Institute of Vertebrate Paleontology and Paleoanthropology, CAS Center for Excellence in Life and Paleoenvironment, Chinese Academy of Sciences, Beijing 100044, China; University of Chinese Academy of Sciences, Beijing 100049, China, liujun@ivpp.ac.cn

ABSTRACT—Dissorophidae are terrestrial temnospondyls with conspicuous armor. All known Guadalupian dissorophid species, including *Anakamacops petrolicus*, are established based on incomplete materials. Here two new dissorophid specimens from the Guadalupian Dashankou Fauna of China are described and referred to *A. petrolicus*. They provide much more new osteological information of this species. *Anakamacops petrolicus* has the largest skull among all known dissorophid species. It exhibits knobby exostoses on the skull roof and mandible, a high suborbital bar that is greater than half of the skull height, a triangular, posteriorly closed otic notch with the anteroposterior length greater than the width, relatively smooth vomer with a few denticles on the lateral margin, two nuchal (occipital) ridges with short overlap where the right one is anterior to the left one, the interpterygoid vacuity far from the choana, low coronoid process, the medial ridge of the adductor fossa close to the ventral margin of the mandible, and the first inner osteoderm nearly triangular with concave margins in dorsal view. The Guadalupian dissorophid species form a monophyletic clade, Kamacopini, which was distributed in northeastern Pangaea, with the following synapomorphies to differentiate it from other dissorophids: suborbital bar high (subequal to or greater than the orbital height) and the interpterygoid vacuities far from the choanae.

## INTRODUCTION

The Olsoniformes are a clade of terrestrial temnospondyls from late Carboniferous and Permian environments (DeMar, 1966; Anderson et al., 2008; Reisz et al., 2009). Within this group, the Dissorophidae are a taxonomically diverse and morphologically distinct clade. These Paleozoic amphibians are characterized by their conspicuous armor (Williston, 1910). Their body lengths generally range from 25 to 50 cm (Schoch and Sues, 2013). Most dissorophid species are known from the Cisuralian (early Permian) of North America (Carroll, 1964; Schoch, 2012), with only five taxa having been reported from the Guadalupian (middle Permian) of Russia and China. In Russia, the first known dissorophid, *Zygosaurus lucius*, was reported from a heavily worn skull (Eichwald, 1848). Later, two taxa, *Kamacops acervalis* and *Iratusaurus vorax*, were established from incomplete skulls, and a fragmentary specimen was tentatively referred to *Alegeinosaurus* (Gubin, 1980, 1993). *Anakamacops petrolicus*, based on a left snout, is the only dissorophid and the only temnospondyl known from the Permian of China (Li and Cheng, 1999). The Guadalupian dissorophids from Russia and China are significantly larger compared with the older ones. The skull of *Z. lucius* measures ca. 17 cm in length and ca. 11 cm in width. The preorbital length is 7 cm in the holotype of *A. petrolicus*, resulting in a complete skull length estimate of greater than 20 cm. The skulls of *K.*

acervalis and *I. vorax* measure ca. 20 cm in width, whereas the skull length of *K. acervalis* was estimated to be 25–30 cm (Gubin, 1980).

A cladistic analysis of the Dissorophidae was initially carried out by Schoch (2012), and more recent studies show that the Dissorophidae include a few basal members and two major clades, the Dissorophinae sensu stricto and the Eucacopinae (Holmes et al., 2013; Schoch and Sues, 2013). The Eucacopinae are characterized by the abbreviated postparietal, the presence of an internarial fenestra, a semilunar curvature on the squamosal, and a transverse ridge on the postparietal (Schoch and Sues, 2013). The two Russian taxa, *Kamacops* and *Zygosaurus*, form a monophyletic clade to the exclusion of *Cacops* (Schoch, 2012). Given that the known materials of *Iratusaurus vorax* (Paleontological Institute, Russian Academy of Sciences, PIN 164/300) and *Anakamacops petrolicus* (Institute of Geology, Chinese Academy of Geological Sciences, IGCAGS V365) are so fragmentary (Gubin, 1980; Li and Cheng, 1999), Schoch (2012) did not include these two taxa in his original phylogenetic matrix. However, *I. vorax* could be referred to a clade including *Cacops*, *Kamacops*, and *Zygosaurus* based on the presence of a closed otic notch.

The Dashankou tetrapod fauna derives from the Qingtoushan Formation of Yumen, Gansu Province, China, and it is dominated by therapsids such as *Sinophoneus yumenensis* Cheng and Ji, 1996, *Biseridens qilianicus* Li and Cheng, 1997, and *Raranimus dashankouensis* Liu, Rubidge, and Li, 2009. The fauna also includes *Belebey chengi* Müller, Li, and Reisz, 2008 (Bolosauridae), *Gansurhinus qingtoushanensis* Reisz, Liu, Li, and

Color versions of one or more of the figures in the article can be found online at www.tandfonline.com/ujvp.

Müller, 2011 (Captorhinidae), *Anakamacops petrolicus* Li and Cheng, 1999 (Dissorophidae), *Yumenerpeton yangi* Jiang, Ji, and Mo, 2017 (Bystrowianidae), *Ingentidens corridoricus* Li and Cheng, 1999, and *Phratochronis qilianensis* Li and Cheng, 1999 (Chroniosuchidae). The age of the fauna is regarded as Roadian (Liu et al., 2009) or Wordian (Rubidge, 2005). Among the previously unstudied materials from this locality are two specimens that can be referred to Dissorophidae. These specimens are larger than all other known dissorophid specimens. Herein, I describe the new specimens, tentatively referring them to *A. petrolicus*, and examine the phylogenetic position of that species among Dissorophidae.

**Institutional Abbreviations**—**IGCAGS**, Institute of Geology, Chinese Academy of Geological Sciences, Beijing, China; **IVPP**, Institute of Vertebrate Paleontology and Paleoanthropology, Chinese Academy of Sciences, Beijing, China; **PIN**, Paleontological Institute, Russian Academy of Sciences, Moscow, Russia.

**Anatomical Abbreviations**—**I**, channel for the olfactory nerve; **V**, recess for exit of trigeminal nerve; **a**, angular; **art**, articular; **bo**, basioccipital; **bs**, basisphenoid; **bt**, basal tubera; **ctf**, chorda tympanic foramen; **d**, dentary; **ec**, ectopterygoid; **eo**, exoccipital; **ep**, epipterygoid; **f**, frontal; **fm**, foramen magnum; **fo**, fenstra ovalis; **imf**, inframeckelian fossa; **j**, jugal; **l**, lacrimal; **lep**, laterally exposed palatine; **m**, maxilla; **mco**, middle coronoid; **nr**, nuchal ridge; **on**, otic notch; **ot**, otic capsule; **p**, parietal; **par**, prearticular; **pco**, posterior coronoid; **pl**, palatine; **po**, postorbital; **pof**, postfrontal; **pop**, paroccipital process; **pp**, postparietal; **prf**, prefrontal; **ps**, parasphenoid; **psl**, postsplenial; **pt**, pterygoid; **ptf**, posttemporal fossa; **q**, quadrate; **qj**, quadratojugal; **qpt**, quadrate ramus of pterygoid; **sa**, suprangular; **sm**, sphenethmoid; **sq**, squamosal; **st**, supratemporal; **t**, tabular; **v**, vomer.

## SYSTEMATIC PALEONTOLOGY

TEMNOSPONDYLI Zittel, 1888
DISSOROPHOIDEA Bolt, 1969
DISSOROPHIDAE Boulenger, 1902
EUCACOPINAE Schoch and Sues, 2013
KAMACOPINI, new taxon

**Definition**—The most inclusive clade that includes *Kamacops acervalis*, but not *Cacops woehri*.

*ANAKAMACOPS PETROLICUS* Li and Cheng, 1999
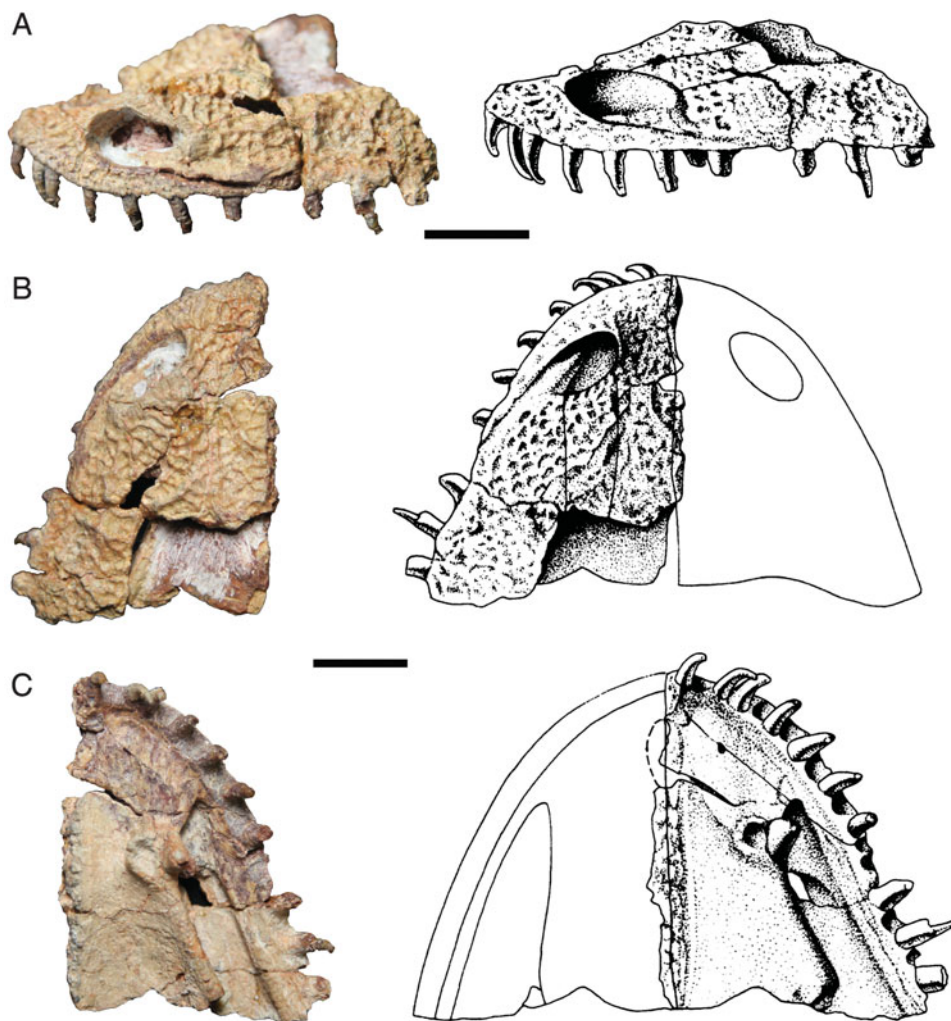(Figs. 1–8)



FIGURE 1. *Anakamacops petrolicus*, IGCAGS V365, holotype. Photos and drawings of the snout in **A**, lateral, **B**, dorsal, and **C**, ventral views. Drawings from Li and Cheng (1999:fig. 3). Scale bars equal 2 cm.

**Holotype**—IGCAGS V365, left side of a snout (Fig. 1).

**Referred Specimens**—IVPP V 23862, an incomplete posterior half of the skull with incomplete lower jaws, an intercentrum, and two osteoderms; IVPP V 23863, posterior end of a right lower jaw.

**Locality and Horizon**—Dashankou locality, Yumen, Gansu Province, China; Qingtoushan Formation (formerly called the Xidagou Formation) (Liu et al., 2012).

**Revised Diagnosis**—Large dissorophid with knobby exostoses on the skull roof and mandible, high suborbital bar with height greater than half of skull height, closed otic notch, interpterygoid vacuity far from choana, coronoid process low, and medial ridge of adductor fossa close to ventral margin of mandible. Potential apomorphies within Dissorophidae: vomer relatively smooth, not shagreen-like, with a few denticles on the lateral margin; two nuchal (occipital) ridges with short overlap and right ridge anterior to the left one; and first internal osteoderm nearly triangular with concave margins in dorsal view. It can be differentiated from other members of Kamacopini (*Zygosaurus*, *Kamacops*, *Iratusaurus*) by otic notch anteroposterior length that is greater than its width.

## DESCRIPTION

### Skull

The skull of IVPP V 23862 is incomplete, missing most of the preorbital portion and the left temporal region. It is quite large, with a maximum width greater than 28 cm. The preserved skull measures ca. 26 cm along the midline, and the complete skull is estimated to have been ca. 40 cm in midline length, based on the skull shape of *Cacops* (Reisz et al., 2009). The skull is relatively wide but low and trapezoid in occipital view, with the cheek at an angle of ca. 130°–140° with the skull table (Figs. 1, 2). The skull was slightly distorted during fossilization. The right side appears to have been compressed to some degree, resulting in the left orbit facing almost laterally, and the right orbit facing more dorsally. The relatively small orbits are oval in outline, bordered by the thickened and elevated circumorbital ridge, which is very prominent in the frontal region.

The skull can be divided into the dorsal (skull table), lateral (cheek), ventral (palate), and occipital (occiput) portions (Fig. 2). Two longitudinal ridges, one anterior to the orbit (prefrontal ridge), another posterior to the orbit (postorbital-squamosal ridge), mark the border between the lateral and dorsal surfaces. Two tall, sharp, transverse nuchal (occipital) ridges lie on the posterior margin of the skull table; the right one is anterior to the left one along the midline. This portion shows no distortion and is in its original shape. The nuchal ridges, formed by the postparietals and tabulars, separate the occipital and the dorsal surface. Medial to the postorbital-squamosal ridge, another ridge extends posteriorly and slightly laterally from the postfrontal to the supratemporal, then it inflects medially on the tabular. This ridge is continuous with the circumorbital ridge.

Sculpturing is widely distributed on the dorsal and lateral surfaces of the skull, and it obscures most sutures. The ornamentation consists of small to relatively large polygonal pits framed by ridges that are raised to form prominent tubercles with rounded tips. Such tubercles are predominantly present in
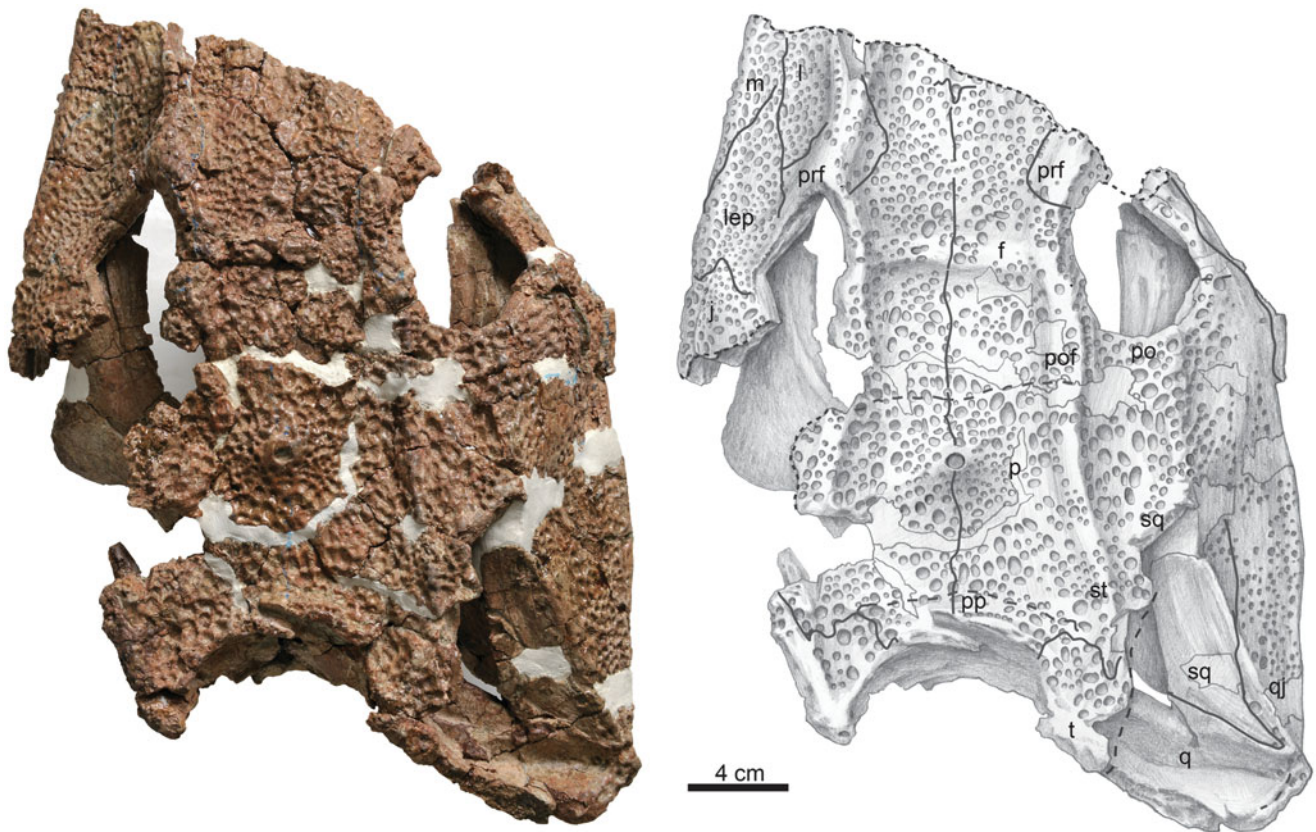


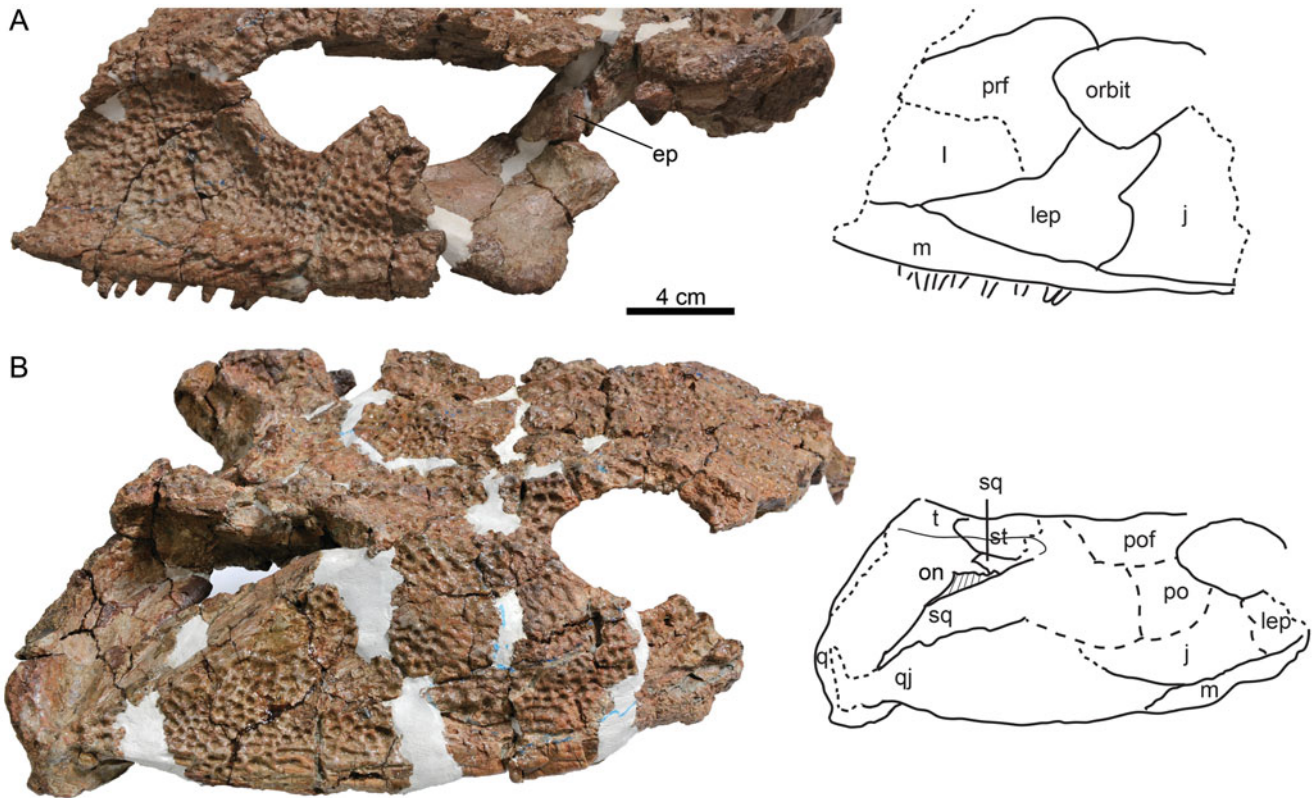FIGURE 2. *Anakamacops petrolicus*, IVPP V 23862. Skull in dorsal view.

FIGURE 3. *Anakamacops petrolicus*, IVPP V 23862. Skull in **A**, left lateral and **B**, dorsolateral views.

the corners of the polygons. This sculpturing pattern is similar to the pattern in other dissorophids such as *Cacops morrisi* and *Kamacops acervalis* (Gubin, 1980; Reisz et al., 2009) but differs from the pattern in trematopids other than *Ecolsonia*, which has no development of protuberances or ridges on the skull table (Berman et al., 1981, 1985).

The skull table is nearly flat except for a down-sloping preorbital portion (Fig. 3). The interorbital region, mostly formed by the frontal, is ca. 8 cm in width, much greater than the orbital diameter (5–6 cm). A transverse ridge connects both orbits within the middle of the interorbital region. The pineal foramen is well developed on a slightly raised area of the skull table, lying closer to the level of the posterior margin of the orbits than to the occipital margin. The posterior border of the skull table is formed by the postparietals and tabulars. The postparietals bear paired posteroventral projections (occipital flanges) that are sutured to the exoccipital.

The preserved left lateral portion of the skull, which is anterior to or below the orbit, bears a large depression formed mainly by the lateral exposure of the palatine (LEP), the lacrimal, and the prefrontal. The preserved right lateral portion, which is mostly posterior to the orbit, is nearly flat. Anterior to the orbit, the prefrontal ridge possibly extends anteriorly to the nasal. The ridge extends posteriorly to join the circumorbital ridge, where the surface sculpturing is coarsest. It appears that the lacrimal does not contribute to the orbital margin as in *Cacops morrisi* (Reisz et al., 2009) (Fig. 3). The suborbital bar is dominated by the large LEP, which is sutured with the prefrontal, the lacrimal, the maxilla, and the jugal, and contributes to the orbital margin. The suborbital bar measures 55 mm in height on the left side and 45 mm on the right side. The height of the suborbital bar is more than half the skull height. This

also is the case in *Kamacops* (Gubin, 1980) and could be related to the large size of the specimen, because the suborbital bar increases in height during ontogeny as shown in *Cacops morrisi* and *Sclerocephalus haeuseri* (Reisz et al., 2009; Schoch and Witzmann, 2009).

The maxilla is excluded from the orbit by the sculptured portion of the palatine on the external surface and the suborbital process of the jugal. The maxilla extends posterior to the posterior border of the ectopterygoid and contacts the quadratojugal (Fig. 4). The left maxillary tooth row preserves eight nearly complete teeth, five roots, and a few empty alveoli, whereas the right row preserves no teeth. All marginal teeth are recurved medially, oval in cross-section, and lack a cutting edge. The last maxillary tooth terminates at the level of the posterior margin of the orbit.

The posterolateral side of the skull is only preserved on the right side, and the sutures are hard to identify (Figs. 2, 3). The exact borders of the postorbital, the jugal, and the quadratojugal are unclear. However, the jugal contributes to the posteroventral margin of the orbit. The quadratojugal forms the posteroventral edge of the skull and seems to extend onto the dorsal process of the quadrate.

The temporal region of the skull is dominated by a closed tympanic embayment, as in the Russian dissorophids (Eichwald, 1848; Gubin, 1980). The supraotic border consists of an anteroposteriorly elongated vertical flange, the supratympanic flange of Bolt (1974) (Fig. 3B), that is formed by the squamosal, the supratemporal, and the tabular. The squamosal and the tabular narrowly contact one another below the supratemporal and exclude the latter from the ventral margin of the flange. Immediately anterior to the level of the squamosal-tabular contact, there is a convex expansion of the ventral
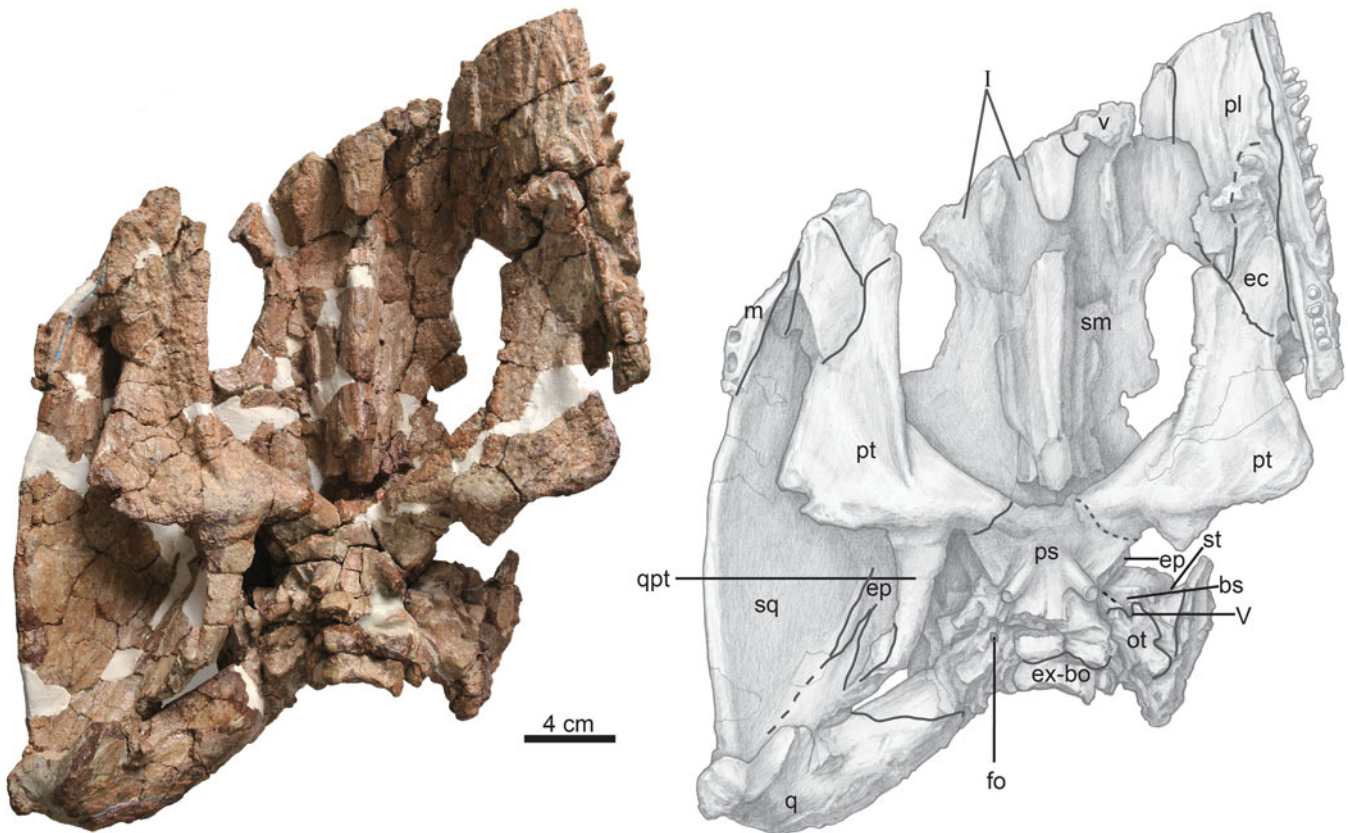
FIGURE 4. *Anakamacops petrolicus*, IVPP V 23862, skull in ventral view.

margin of the flange, the 'semilunar curvature' of Bolt (1974), which projects slightly laterally. The sculptured surface of the skull table laterally overhangs the dorsal margin of the smooth, anterior portion of the supratympanic flange in the form of a narrow, lip-like structure, termed the supratympanic shelf. The shelf seems to extend posteriorly along the entire length of the dorsal margin of the smooth supratympanic flange.

The tabular has a ventral projection, which is directed toward the quadrate (Figs. 3, 5). The quadrate has a large, mediolaterally expanded dorsal process that is fused to the tabular, thus closing the otic notch posteriorly. The dorsal margin of the tabular-quadrate complex is broken. The quadrate bears a thick crest on its lateral side that is continuous with a ridge of the quadratojugal. The quadrate condyle is massive and bears a saddle-shaped, double-keeled articular surface. The quadrate sends two processes anteriorly: a dorsal one that contacts the epipterygoid and a ventral one that contacts the quadrate process of the pterygoid (Fig. 4).

The ventral margin of the right otic notch is a laterally tilted unornamented shelf, which is almost entirely formed by the squamosal (Figs. 2, 3). The shelf slopes posteroventrally at ca. 25° from the horizontal, but this measurement is likely an underestimate given the dorsoventral postmortem crushing of the skull. The squamosal shelf is attached along its medial edge by the quadrate ramus of the pterygoid and the epipterygoid, along its lateral edge by the dorsal side of the quadratojugal, and along its posterior edge by the quadrate.

The occipital condyle is bipartite, with two vertical oval condylar facets formed almost completely by the exoccipital (Figs. 4, 5). The arc-shaped basioccipital sheaths the exoccipitals ventrally. The sutures between the basioccipital and exoccipitals are not discernible. Dorsolateral to the occipital condyle, the exoccipital has a large, smoothly concave surface, which should be an attachment site for a nuchal ligament. The suture between the exoccipital and the paroccipital process is not clear. Dorsomedially, two exoccipitals suture with the postparietal and meet along the midline dorsal to the foramen magnum. The ossified synotic tectum, supraoccipital, is not identified here as in dissorophoids in general, although it was reported in *Dissorophus angustus* (Carroll, 1964) and *Kamacops acervalis* (Schoch, 1999). The postparietal is quite tall, with a height nearly half the height of the occiput.

The small foramen magnum lies completely within the two exoccipitals in occipital view (Fig. 5). The posttemporal fossa is low and wide, with an irregular shape. The fossa is bordered by the tabular laterally, the postparietal dorsally and medially, and the paroccipital process ventrally. Its ventral floor is almost completely formed by the paroccipital process.

The prootic and opisthotic are fused, forming a single otic capsule (Fig. 4) that is articulated to the basisphenoid anteriorly, the supratemporal anterolaterally, and the tabular laterally with a rounded surface. The element extends laterally well beyond the postparietal-tabular suture. At the proximal end of the otic lies the fenestra ovalis, which is not well preserved. The anteromedial edge of the otic bears a large recess through which the trigeminal nerve must have passed.

The braincase is ensheathed ventrally by the parasphenoid. The basisphenoid lies dorsal to the parasphenoid body but cannot be differentiated from it. The basal plate is approximately rectangular, and its ventral surface directed anterodorsally, forming an obtuse angle with the long cultriform process (Fig. 4). On the posterior margin of the basal plate, the basal
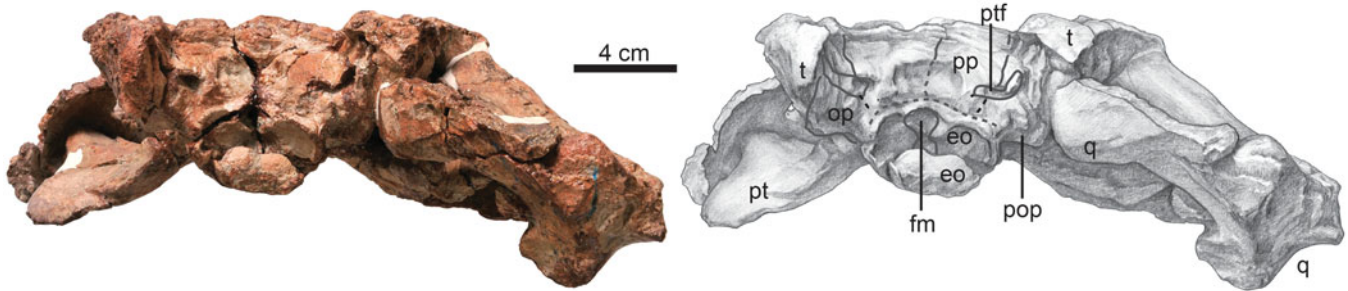
FIGURE 5. *Anakamacops petrolicus*, IVPP V 23862, skull in occipital view.

tubera extends well posteriorly and the basioccipital has a short ventral exposure. Two ridges extend posterolaterally on the ventral surface of the body. The upturned posterolateral corner forms part of the margin of the fenestra ovalis. The basipterygoid process is thick, long, and directed anteroventrally rather than directly laterally. The cultriform process is narrow and round in cross-section, and only slightly expanded near the anterior end. Although the tip is missing, the process extends anteriorly to or beyond the level of the anterior margin of the interpterygoid vacuities.

The basicranial region is similar to that of the late Permian *Kamacops* in the proportions of the basal plate and in the length of the basipterygoid process (Schoch, 1999). The basipterygoid process extends laterally to suture with the epipterygoid dorsally and the pterygoid ventrally. The incomplete left epipterygoid is exposed dorsally (Fig. 3A), and the right one can be observed anteriorly and laterally (Fig. 4). The epipterygoid has an extensive footplate (processus basalia of Schoch, 1999) attaching to the basipterygoid branch of the pterygoid. The epipterygoid extends toward the skull roof to touch the squamosal.

The sphenethmoid is 'V'-shaped in cross-section, and it is partially covered ventrally by the cultriform process of the parasphenoid and capped dorsally by the skull roof (Fig. 4). The sphenethmoid is laterally expanded in its anterior portion. Its posterior portion presumably contained the cerebral hemisphere and the olfactory bulbs. The anterior part of the bone is broken, exposing paired tubular channels for the nerve. A ridge, formed by the ventral extension of the frontal, separates the two channels. In living amphibians, the olfactory nerve is divided into the ramus profundus and the ramus dorsalis; the former enters the olfactory lobe proper, and the latter extends into the vomeronasal organ (Duellman and Trueb, 1994; Maddin et al., 2012). Here, the two channels are interpreted as channels for the two branches of the olfactory nerve (the medial one to the olfactory lobe proper and the lateral to the vomeronasal organ).

The pterygoid is a massive bone on the palate. It can be divided into three components: a horizontally expanded palatal ramus, a vertically ascending quadrate ramus, and a thickened medial area in the region of the basal articulation with the braincase. The quadrate ramus extends dorsally to the squamosal and completely encloses the internal portion of the cheek. The palatal ramus forms a pronounced transverse flange, giving the lateral corner a nearly rectangular shape. It descends below the level of the palate and is directed ventrolaterally. The pterygoid is the major contributor to the lateral border of the interpterygoid vacuity. The interpterygoid vacuities are large, nearly trapezoid in outline, and their width decreases slightly posteriorly.

The ectopterygoid is a quadrilateral bone between the pterygoid, the palatine, and the maxilla. The border between the ectopterygoid and the palatine is not clear, but here two fangs are identified on the anterior side of the ectopterygoid. Fangs on the ectopterygoid are also observed in *Broiliellus reiszi* (Holmes et al., 2013) and *Cacops woehri* (Fröbisch and Reisz, 2012). Medial and slightly posterior to the last fang, it seems that there is the root of a fang on the posterior process of the palatine. It is unknown in other dissorophids. The palatine is positioned on the anterolateral side of the interpterygoid vacuity, and its posterior end wedges slightly between the pterygoid and the ectopterygoid as in *Reiszerpeton* (Maddin et al., 2013). The posterior margin of the choana should be formed by the anterolateral side of the palatine, and two fangs are usually present posterior to the choana (Schoch, 2012). This portion of the palatine is not preserved, but the preserved palatine indicates that the posterior margin of the choanae is far from the anterior margin of the interpterygoid vacuities, similar only to *Kamacops* among dissorophids (Gubin, 1980; Schoch, 2012). The palatine has a large laterally exposed portion and is ornamented just like the surrounding skull roof bones in adults.

The left vomer is partially preserved anterior to the interpterygoid vacuity and is bordered laterally by the palatine. The ventral surface of the vomer is relatively smooth, not shagreen-like, but a few indistinct round denticles are present along the lateral side. The pterygoid, ectopterygoid, and palatine are densely covered by denticles, and the denticles on the medial margin of the pterygoid are more prominent. There is no denticle field on the parasphenoid.

## Mandible

The mandible of IVPP V 23862 is preserved, including the posterior portion of the left ramus and the right ramus missing the symphysis and posterior end (Fig. 6). The complete lower jaw should be more than 40 cm in length. The posterior portion of another right mandibular ramus (IVPP V 23863) is also present (Fig. 7). The following description is almost completely based on IVPP V 23862.

The anterior part of the right mandibular ramus is crushed and distorted, and the original bone surface is poorly preserved. The upper margin of the jaw should form a roughly straight line, corresponding to the straight upper jaw. The jaw bends medially posterior to the inframeckelian fossa, resulting in the adductor fossa being positioned beneath the subtemporal fossa.

The dentary is elongated, the largest bone of the lower jaw, and mainly exposed on the lateral surface (Fig. 6B, C). The anterior end of the dentary is missing. It extends posteriorly as a long and sharp process, which lies above the angular and ends within the surangular. The lateral surface of the dentary is smooth, lacking the ornamentation present on the angular. The dorsal surface of the dentary has a
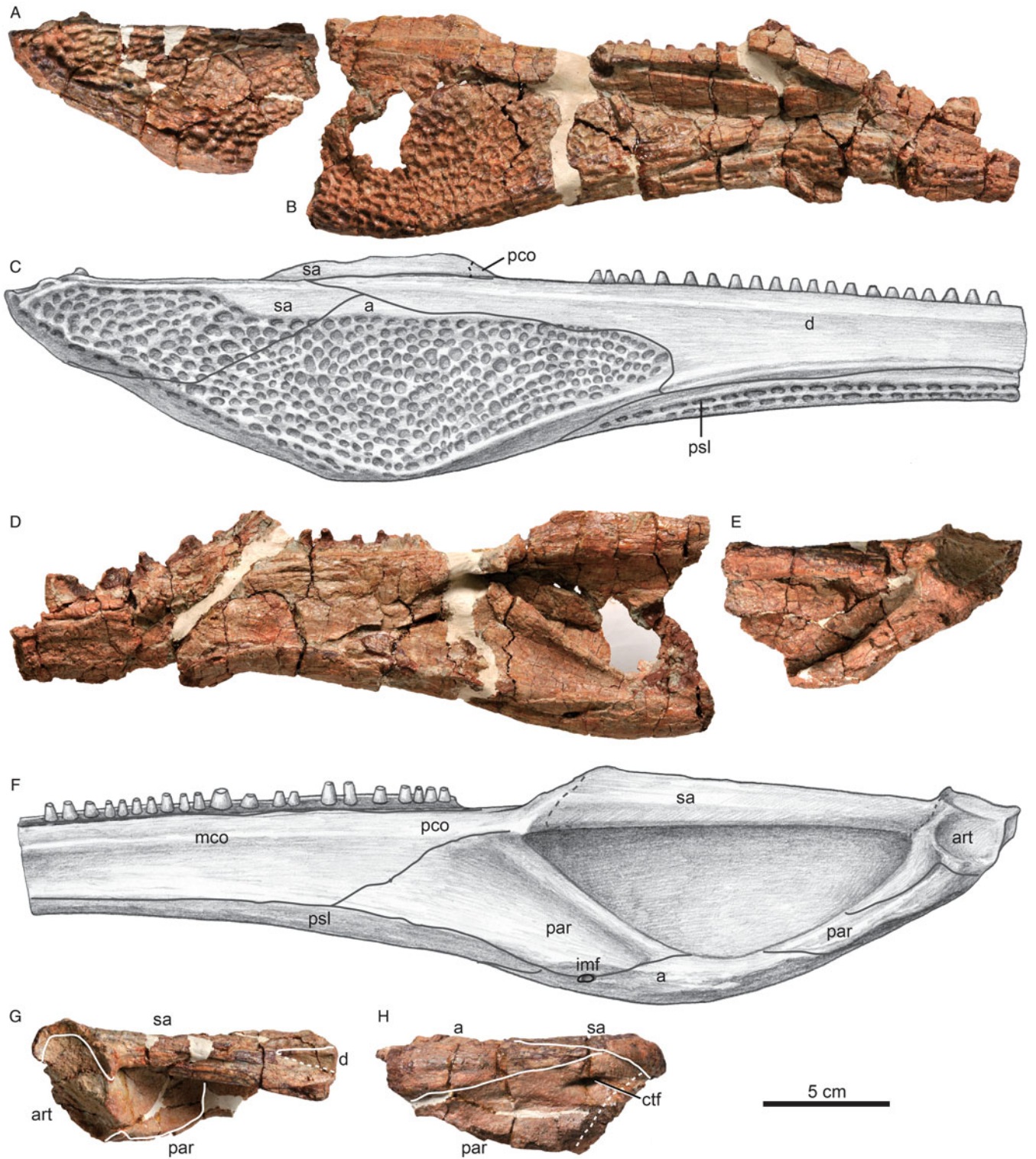
FIGURE 6. *Anakamacops petrolicus*, IVPP V 23862, mandible. **A**, left mandibular ramus in lateral view (reversed as right side). **B**, right mandibular ramus in lateral view. **C**, reconstruction of mandible in right lateral view. **D**, right mandibular ramus in medial view. **E**, left mandibular ramus in medial view (reversed as right side). **F**, reconstruction of right mandibular ramus in medial view. Posterior end of left ramus in **G**, dorsal and **H**, ventral views.

furrow that extends the length of the element between the dentary teeth and the raised edge of the coronoids. This furrow most likely held the dental lamina. There are 15 preserved dentary teeth, and their shape is identical to that of the maxillary teeth. The posterior two teeth are smaller than the anterior teeth.
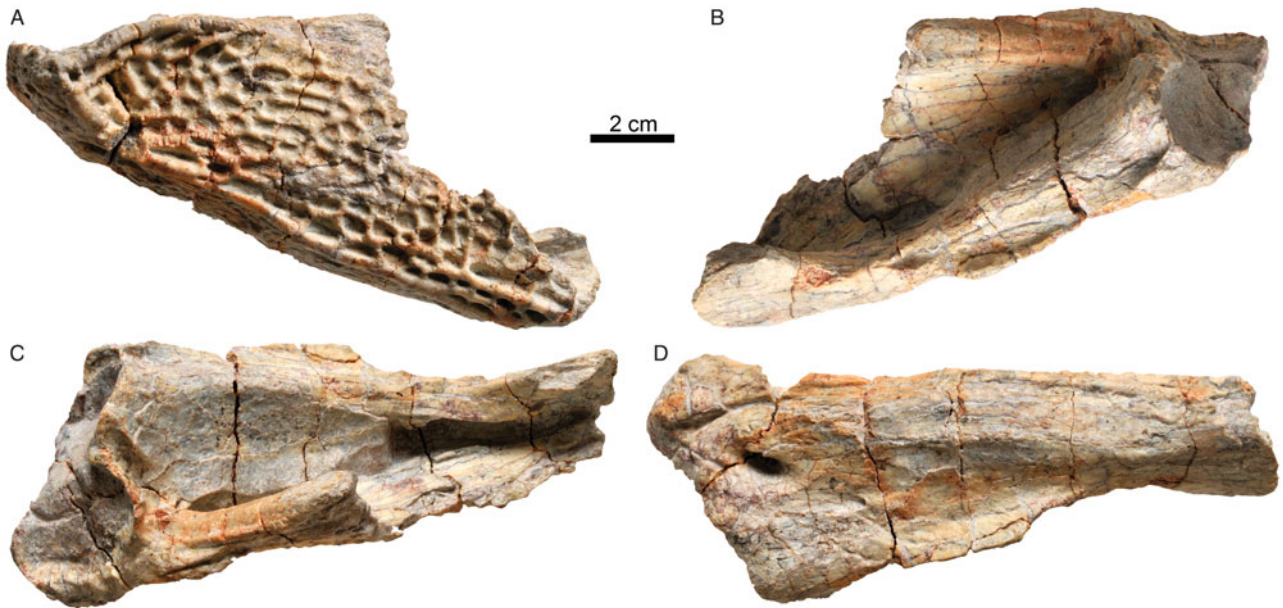
FIGURE 7. *Anakamacops petrolicus*, IVPP V 23863, mandible. Posterior end of right ramus in **A**, lateral, **B**, medial, **C**, dorsal, and **D**, ventral views.

The splenial is not preserved. The postsplenial forms most of the floor of the Meckelian canal (Fig. 6B–F). It extends posteriorly and terminates slightly anterior to the inframeckelian fossa. It has more exposure on the lateral surface than on the medial surface.

The angular is a large bone on the posteroventral corner of the mandible (Fig. 6A–C), and it forms the lateral edge of the adductor fossa with the surangular. It has an anterior process inserting between the dentary and the postspenial on the lateral surface. The lateral surface of the angular is ornamented with pits and ridges, which continue as distinct ridges on the posteroventral margin. On the ventral surface, it is sutured with the prearticular and occupies the lateral side of the ventral plate (Fig. 6H).

The right surangular is broken, but the left one is nearly complete (Fig. 6A). Its dorsal margin is thickened medially to cover the adductor fossa. The suture between the surangular and the angular is a concave line on the lateral surface, which extends anterodorsally to meet the dentary. The suture extends backward and downward to the ventral surface (Fig. 6H). The bone covers the lateral side of the articular, and the latter is not observed in lateral view (Fig. 6A, G).

The coronoids form most of the medial surface of the mandible (Fig. 6D). Some denticles are present on the middle portion, but not the posterior portion, of the coronoids. The boundaries between coronoids are not clear. According to other dissorophids such as *Broiliellus reiszi* (Holmes et al., 2013), three coronoids are expected in this species. Posteriorly, the posterior coronoid extends to the anterior corner of the adductor fossa to fuse with the dorsomedial surface of the surangular. The coronoid process is poorly developed, in contrast to the high crest in dissorophids such as *Broiliellus* and *Dissorophus* (DeMar, 1968; Holmes et al., 2013). It is more similar those of *Cacops morrisi* (Gee and Reisz, 2018) and trematopids such as *Phonerpeton* (Dilkes, 1990). The medial surface of the coronoid flange is thickened greatly in a fashion similar to that of the surangular and has a pronounced pocket that opens posterodorsally.

The prearticular is restricted to the ventromedial side of the mandible (Figs. 6, 7). It forms most of the medial wall of the adductor fossa and ends dorsally in a free medial rim. The medial wall of the adductor fossa is low, with the lowest point close to the ventral margin of the mandible, so the adductor fossa has a large medial exposure. In *Broiliellus* and *Dissorophus*, the medial wall of the adductor fossa is around the level of the tooth row, so the adductor fossa only has a much smaller medial exposure (DeMar, 1968; Holmes et al., 2013). The prearticular expands medially under the posterior portion of the adductor fossa, so the width of the lower jaw in this region is greater than two times that of the anterior width (Figs. 6H, 7D). Ventral and roughly parallel to the beveled rim of the adductor fossa, a narrow flange delineates the insertion along the medial rim for the adductor mandibulae internus muscle (Adams, 1919).

The articular is well exposed dorsally as a glenoid for the quadrate condyle (Figs. 6, 7). The glenoid is subdivided into two parts by an anteroposterior ridge, with the lateral part nearly horizontal and the medial ventrally sloping. Anteriorly, the articular extends as a flattened, nearly trapezoid process well anterior within the floor of the adductor fossa (Figs. 6G, 7C). The margins of this process are well defined. The anterior margin is a nearly straight line, rather than a narrow tip. Anteriorly, the articular should be continued by the Meckelian cartilage. It is sheathed ventrally by the prearticular and the angular.

A large, oval opening, the chorda tympanic foramen (para-articular foramen of Romer and Witter, 1942) for the chorda tympani branch of cranial nerve VII and associated blood vessels, is located near the posterior margin on the ventral surface (Figs. 6H, 7D). This foramen lies within the prearticular on the ventral surface, and without the contribution of the surangular as in *Acheloma dunni* (Polley and Reisz, 2011). Dorsally, it lies between the surangular and the articular within the adductor fossa. Anterior to the chorda tympanic foramen, a tiny oval foramen opens posteriorly on the posterior portion of the prearticular (Fig. 7D).
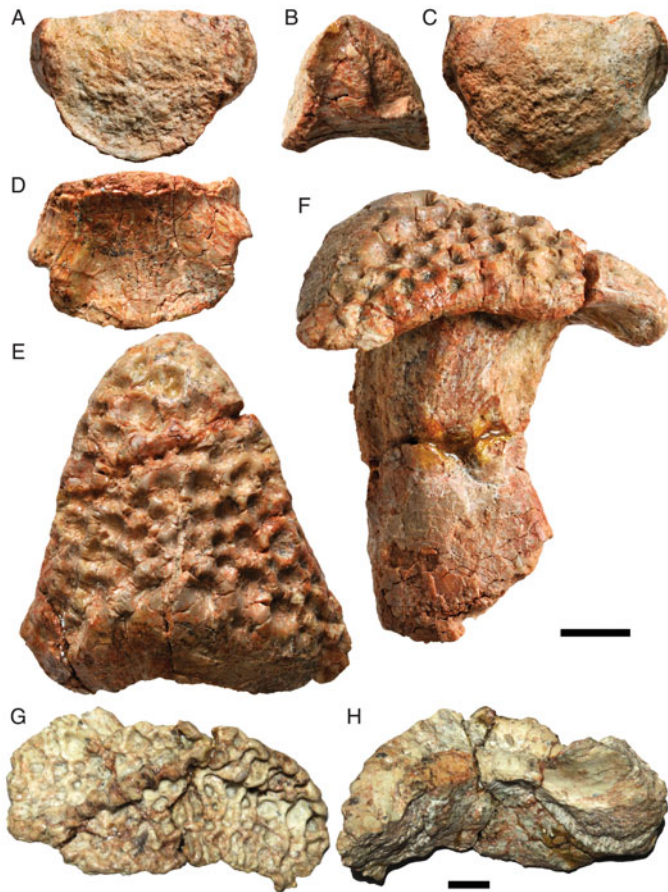
FIGURE 8. *Anakamacops petrolicus*, IVPP V 23862. An intercentrum in **A**, anterior, **B**, lateral, **C**, posterior, and **D**, ventral views. The first internal osteoderm in **E**, dorsal and **F**, right lateral views. An external osteoderm in **G**, dorsal and **H**, ventral views. Scale bars equal 1 cm.

**Postcranial Elements**

One intercentrum and two osteoderms were prepared from the same packet as the skull, and they are assumed to belong to the same individual as the skull (IVPP V 23862). The intercentrum agrees with the crescentric, laterally wedge-shaped morphology that is common for rhachitomous temnospondyls (Fig. 8A–D). The lateral and ventral surfaces are covered with smooth periosteal bone. A subcircular unfinished area is present along the posterior margin for articulation with the capitulum of the rib. The ventral middle part is a smooth, low ridge, and its two sides are slightly concave. The anterior surface is nearly flat, and the posterior one is convex.

One osteoderm is identified as the first internal osteoderm, and the other is tentatively identified as an incomplete external osteoderm. The internal osteoderm is fused to the robust neural spine as in *Aspidosaurus* and *Cacops* (Fig. 8E, F) (DeMar, 1966). The neural spine expands distally along the midsagittal and transverse planes, with anterior and posterior edges, as in *Cacops aspidephorus* (Dilkes, 2009). The internal osteoderm is subtriangular in dorsal profile, formed by two obtuse triangles, whose posterior margins form an angle of 95°. Its anteroposterior length is slightly greater than the transverse width, closer to the condition in *Cacops* than *Dissorophus* (DeMar, 1966). The lateral margins are concave rather than convex, differing from those of other dissorophids (DeMar, 1966). The dorsal surface of the internal osteoderm is ornamented by pits and ridges, similar to the skull roof. The posterior margin of the internal osteoderm, where the external osteoderm overlaps it, is ventrally slanted and smooth.

The external osteoderm is only preserved on one side, and a slanting ridge divides its dorsal and lateral surfaces (Fig. 8G, H). One margin is raised as a ridge, and a concave facet lies beneath this margin, likely the articular surface for an adjacent osteoderm. The ventral surface of another margin is poorly preserved, but the elongation on the medial part looks like cover of the next osteoderm.

DISCUSSION

The skull represents the adult stage of its species. Other than exhibiting the largest size among all known dissorophids, it is well ossified, with well-developed sculpturing (Steyer, 2000). The neurocranium also shows most features of the later ontogenetic stages of *Acheloma*, such as the exoccipitals meeting at midline, completion of basal tubera, completion of paroccipitals, and a tall postparietal (Maddin et al., 2010).

Specimen IVPP V 23683 is identified as same taxon as IVPP V 23682 on the basis of the comparable structure of the posterior mandible. Specimen IVPP V 23682 is diagnosed as a member of Olsoniformes by the presence of a tabular meeting the squamosal; the squamosal having a dorsally exposed and ornamented area (supratympanic flange) stepping abruptly into a steeply aligned, poorly ornamented portion; a supratemporal forming a marked ventral flange participating in the medial bordering of the otic notch; and a cultriform process that is thin and round in cross-section (Schoch, 2012). The fossils clearly are not trematopids because the ventral surface of the parasphenoid lacks denticles and the vomer is excluded from the pterygoid by the palatine. However, they can be referred to the Dissorophidae by the presence of maxillary teeth terminating at the level of the posterior margin of the orbit, a basipterygoid articulation firmly sutured at midlevel of the widened basipterygoid process, and a smooth basal plate of the parasphenoid (Schoch, 2012).

One dissorophid taxon, *Anakamacops petrolicus*, was named on the basis of a left snout (IGCAGS V365) from the same locality (Fig. 1). Although based on fragmentary material, this taxon is valid. The ventral surface of vomer is relatively smooth, bearing no shagreen of teeth, only a few denticles on the lateral margin. This feature is not observed in other known dissorophids (Li and Cheng, 1999). Although the new specimens do not exhibit overlapping morphology with the holotype (IGCAS V365) and their sizes differ, they can be referred to *A. petrolicus* based on the unique feature of the vomer and the following cladistic analysis.

To test the relationships of the new specimens and the holotype of *Anakamacops petrolicus*, they were coded separately into a revised character matrix based on Holmes et al. (2013) (Appendix 1). Given that the subnarial lacrimal process is almost always absent in dissorophids, a new state is added (character 49). Because no complete skull is known for some species, the suborbital bar height is redefined as relative to orbital height, not relative to skull length (character 53). There were only two defined character states for characters 58 and 67 of Schoch (2012), but three states were coded (although the third state could be known from his explanation). *Conjunctio multidens* is coded from both the holotype and the referred specimen ('RioArriba taxon' of Schoch, 2012). The codings for *Kamacops* and *Zygosaurus* for character 54 (minimum distance from otic notch to posterior orbital margin) were changed from '2' to '1.' *Reiszerpeton renascentis* was referred to Dissorophidae (Maddin et al., 2013), so it also is included here
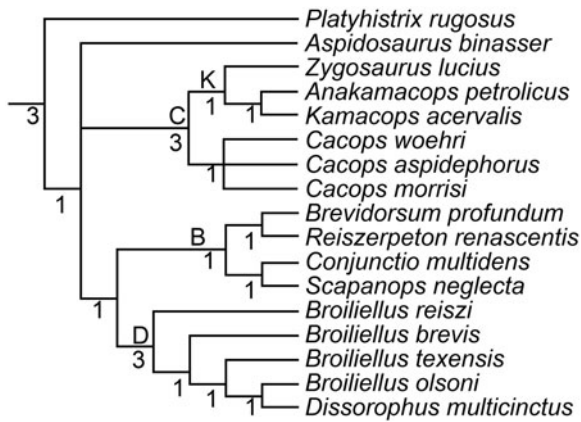
FIGURE 9. Strict consensus tree of six MPTs using a modified version of the data matrix of Holmes et al. (2013), showing the interrelationships within Dissorophoidae, with C = Eucacopinae, D = Dissorophinae, and K = Kamacopini. Numbers below the nodes are the Bremer support values. Common synapomorphies for C: 46(2), 48(1), 63(1); K: 53(1); B + D: 22(1); B: 39(1); D: 13(1), 64(1), 67(1), 71(1).

based on the illustration and description. Hence, the matrix comprises 29 taxa and 71 characters (Supplementary Data 1). The matrix was analyzed with TNT 1.5 (Goloboff and Catalano, 2016) with *Dendrerpeton acadianum* as outgroup and all characters treated as unordered. The parsimony analysis is performed in the heuristic search mode under the default traditional search option, and then a second time with starting trees from RAM. The analysis yielded 2,935 most parsimonious trees (MPTs), each with a length of 142 steps. In 59% of MPTs, IGCAGS V365 and IVPP V 23862 formed a clade. However, in other MPTs, IGCAGS V365 forms a clade with *Zygosaurus*. This result shows that it is reasonable to refer the new specimens to *A. petrolicus*.

*Anakamacops petrolicus* shows the following features unknown in other dissorophids: a relatively smooth vomer that is not shagreen-like, although a few denticles grow on the lateral margin; two nuchal (occipital) ridges with short overlap and the right one anterior to the left one; the coronoid process low; the medial ridge of the adductor fossa close to the ventral margin of the mandible; and the first inner osteoderm nearly triangular with concave margins in dorsal view. Due to the poor preservation in some dissorophid species, some of these characters may be present in other species and may not be identified as apomorphies here.

When *A. petrolicus* is coded for all available specimens (Supplementary Data 2), and the matrix is analyzed with TNT 1.5 (Goloboff and Catalano, 2016) following the previous settings, the analysis produced 1759 MPTs, each with a length of 143 steps. Their topology is similar to the previous results, and both Dissorophinae and Eucacopinae sensu stricto are well supported (Schoch, 2012; Holmes et al., 2013; Schoch and Sues, 2013), but the positions of *Aspidosaurus*, *Brevidorsum*, *Conjunctio*, *Reiszerpeton*, and *Scapanops* are unresolved. When characters 39, 49, 52, 53, and 54 are set as additive, the analysis produced six MPTs, each with a length of 144 steps. The interrelationships within Dissorophidae are well resolved other than *Aspidosaurus* (Fig. 9). Dissorophidae includes two well-supported clades (Dissorophinae, Eucacopinae) (Bremer support value =3) and a new clade (clade B in Fig. 9). Clade B is the sister group of Dissorophinae rather than Eucacopinae. *Aspidosaurus* is found in an early-diverging position on three

MPTs but is the sister taxon of Eucacopinae sensu stricto in the other three MPTs.

*Anakamacops petrolicus* lies within a strict Eucacopinae (Fig. 9), and this clade is supported by the following characters: the tabular process is fused to the quadrate process; knobby exostoses are present on the skull roof; and the carotid artery lies at the base of cultriform process. *Anakamacops* further forms a monophyletic clade (Kamacopini; clade K in Fig. 9) with the Russian *Kamacops* and *Zygosaurus*. One synapomorphy of that clade is a high suborbital bar that is subequal to or higher than the orbital height, so the orbital margin is elevated and the orbit faces more dorsally. This feature can differentiate this clade from all other dissorophids. Another possible synapomorphy of Kamacopini is the interpterygoid vacuity far posterior to the choana, which is present in *Anakamacops* and *Kamacops*, but unknown in *Zygosaurus*. The anterior margins of the interpterygoid vacuities are nearly at the same level of the posterior margins of the choanae in *Platyhystrix rugosus* (Berman et al., 1981), *Cacops aspidephorus* (Williston, 1910), *C. morrisi* (Reisz et al., 2009), and *C. woehri* (Fröbisch and Reisz, 2012); slightly posterior to the posterior margins of the choanae in *Aspidosaurus binasser* (Berman and Lucas, 2003) and *Broiliellus reiszi* (Holmes et al., 2013); and anterior to the posterior margin of the choanae in *Dissorophus multicinctus* and *Broiliellus brevis* (Schoch, 2012). Kamacopini represents a Guadalupian radiation of dissorophids in the northeastern part of Pangaea. This clade may also include *Iratusaurus*.

Within Kamacopini, *Anakamacops* can be differentiated from other genera (*Zygosaurus*, *Kamacops*, *Iratusaurus*) by the shape of the closed otic notch, which is triangular, with the anteroposterior length greater than the width. *Anakamacops* is more closely related to *Kamacops* than *Zygosaurus*. The synapomorphies of *Anakamacops* plus *Kamacops* include a suborbital bar that is greater than half of the skull height and an interorbital region that is wider than the orbit.

LITERATURE CITED

Adams, L. A. 1919. A memoir on the phylogeny of the jaw muscles in recent and fossil vertebrates. Annals of the New York Academy of Sciences 28:51–166.

Anderson, J. S., A. C. Henrici, S. S. Sumida, T. Martens, and D. S. Berman. 2008. *Georgenthalia clavinasica*, a new genus and species of dissorophoid temnospondyl from the Early Permian of Germany, and the relationships of the family Amphibamidae. Journal of Vertebrate Paleontology 28:61–75.

Berman, D. S., and S. G. Lucas. 2003. *Aspidosaurus binasser* (Amphibia, Temnospondyli), a new species of Dissorophidae from the Lower Permian of Texas. Annals of Carnegie Museum 72:241–262.

Berman, D. S., R. R. Reisz, and D. A. Eberth. 1985. *Ecolsonia cutlerensis*, an Early Permian dissorophid amphibian from the Cutler Formation of north-central New Mexico. New Mexico Bureau of Mines and Mineral Resources, Socorro, New Mexico.

Berman, D. S., R. R. Reisz, and M. A. Fracasso. 1981. Skull of the Lower Permian dissorophid amphibian *Platyhystrix rugosus*. Annals of Carnegie Museum 50:391–416.

Bolt, J. R. 1969. Lissamphibian origins: possible protolissamphibian from the Lower Permian of Oklahoma. Science 166:888–891.

Bolt, J. R. 1974. A trematopsid skull from the Lower Permian, and analysis of some characters of the dissorophoid (Amphibia: Labyrinthodontia) otic notch. Fieldiana: Geology 30:67–79.

Boulenger, G. A. 1902. Amphibia; pp. 381–384 in Encyclopedia Britannica, tenth edition. Adam and Charles Black, London.

Carroll, R. L. 1964. Early evolution of the dissorophid amphibians. Bulletin of the Museum of Comparative Zoology 131:161–250.

Cheng, Z., and S. Ji. 1996. First record of a primitive anteosaurid dinocephalian from the Upper Permian of Gansu, China. Vertebrata PalAsiatica 34:123–134.

DeMar, R. E. 1966. The phylogenetic and functional implications of the armor of the Dissorophidae. Fieldiana: Geology 16:55–88.

DeMar, R. E. 1968. The Permian labyrinthodont amphibian *Dissorophus multicinctus*, and adaptations and phylogeny of the family Dissorophidae. Journal of Paleontology 42:1210–1242.

Dilkes, D. W. 1990. A new trematopsid amphibian (Temnospondyli: Dissorophoidea) from the lower Permian of Texas. Journal of Vertebrate Paleontology 10:222–243.

Dilkes, D. W. 2009. Comparison and biomechanical interpretations of the vertebrae and osteoderms of *Cacops aspidephorus* and *Dissorophus multicinctus* (Temnospondyli, Dissorophidae). Journal of Vertebrate Paleontology 29:1013–1021.

Duellman, W. E., and L. Trueb. 1994. Biology of Amphibians. The Johns Hopkins University Press, Baltimore, Maryland, 696 pp.

Eichwald, E. D. 1848. Über die Saurier des kupferführenden Zechsteins Russlands. Bulletin de la Société Impériale des naturalistes de Moscou 21:136–204.

Fröbisch, N. B., and R. R. Reisz. 2012. A new species of dissorophid (*Cacops woehri*) from the Lower Permian Dolese Quarry, near Richards Spur, Oklahoma. Journal of Vertebrate Paleontology 32:35–44.

Gee, B. M., and R. R. Reisz. 2018. Cranial and postcranial anatomy of *Cacops morrisi*, a eucacopine dissorophid from the early Permian of Oklahoma. Journal of Vertebrate Paleontology. doi: 10.1080/02724634.2018.1433186.

Goloboff, P. A., and S. Catalano. 2016. TNT, version 1.5, with a full implementation of phylogenetic morphometrics. Cladistics 32: 221–238.

Gubin, Y. M. 1980. New Permian dissorophids of the Ural forelands. Paleontological Journal 14:88–96.

Gubin, Y. M. 1993. New data on lower tetrapods from the Upper Permian of northern Cis-Urals and Obshchy Syrt. Paleontologischeskii Zhurnal 1993:97–105.

Holmes, R., D. S. Berman, and J. S. Anderson. 2013. A new dissorophid (Temnospondyli, Dissorophoidea) from the Early Permian of New Mexico (United States). Comptes Rendus Palevol 12:419–435.

Jiang, S., S.-a. Ji, and J. Mo. 2017. First record of bystrowianid chroniosuchians (Amphibia: Anthracosauromorpha) from the Middle Permian of China. Acta Geologica Sinica English Edition 91:1523–1529.

Li, J.-L., and Z.-W. Cheng. 1997. First discovery of eotitanosuchian (Therapsida, Synapsida) of China. Vertebrata PalAsiatica 35: 268–282.

Li, J.-L., and Z.-W. Cheng. 1999. New anthracosaur and temnospondyl amphibians from Gansu, China – the fifth report on Late Permian Dashankou lower tetrapod fauna. Vertebrata PalAsiatica 37: 234–247.

Liu, J., B. Rubidge, and J. Li. 2009. New basal synapsid supports Laurasian origin for therapsids. Acta Palaeontologica Polonica 54: 393–400.

Liu, J., Q.-H. Shang, K.-Q. Sun, and L. Li. 2012. The vertebrate fossil-bearing horizon in Yumen, Gansu and the Permian–Triassic strata in north Qilian area. Vertebrata PalAsiatica 50:373–381.

Maddin, H. C., F. A. Jenkins Jr., and J. S. Anderson. 2012. The braincase of *Eocaecilia micropodia* (Lissamphibia, Gymnophiona) and the origin of caecilians. PLoS ONE 7:e50743.

Maddin, H. C., N. B. Fröbisch, D. C. Evans, and A. R. Milner. 2013. Reappraisal of the Early Permian amphibamid *Tersomius texensis* and some referred material. Comptes Rendus Palevol. 12:447–461.

Maddin, H. C., R. R. Reisz, and J. S. Anderson. 2010. Evolutionary development of the neurocranium in Dissorophoidea (Tetrapoda: Temnospondyli), an integrative approach. Evolution & Development 12:393–403.

Müller, J., J.-L. Li, and R. Reisz. 2008. A new bolosaurid parareptile, *Belebey chengi* sp. nov., from the Middle Permian of China and its paleogeographic significance. Naturwissenschaften 95:1169–1174.

Polley, B. P., and R. R. Reisz. 2011. A new Lower Permian trematopid (Temnospondyli: Dissorophoidea) from Richards Spur, Oklahoma. Zoological Journal of the Linnean Society 161:789–815.

Reisz, R. R., R. R. Schoch, and J. S. Anderson. 2009. The armoured dissorophid *Cacops* from the Early Permian of Oklahoma and the exploitation of the terrestrial realm by amphibians. Naturwissenschaften 96:789–796.

Reisz, R. R., J. Liu, J. Li, and J. Müller. 2011. A new captorhinid reptile, *Gansurhinus qingtoushanensis*, gen. et sp. nov., from the Permian of China. Naturwissenschaften 98:435–441.

Romer, A. S., and R. V. Witter. 1942. *Edops*, a primitive rhachitomous amphibian from the Texas red beds. Journal of Geology 50:925–960.

Rubidge, B. S. 2005. Re-uniting lost continents - Fossil reptiles from the ancient Karoo and their wanderlust. South African Journal of Geology 108:135–172.

Schoch, R. R. 1999. Studies on braincases of early tetrapods: structure, morphological diversity, and phylogeny. 2. *Kamacops acervalis* and other advanced dissorophoids. Neues Jahrbuch für Geologie und Paläontologie, Abhandlungen 213:289–312.

Schoch, R. R. 2012. Character distribution and phylogeny of the dissorophid temnospondyls. Fossil Record 15:121–137.

Schoch, R. R., and H.-D. Sues. 2013. A new dissorophid temnospondyl from the Lower Permian of north-central Texas. Comptes Rendus Palevol 12:437–445.

Schoch, R. R., and F. Witzmann. 2009. Osteology and relationships of the temnospondyl genus *Sclerocephalus*. Zoological Journal of the Linnean Society 157:135–168.

Steyer, J. S. 2000. Ontogeny and phylogeny in temnospondyls: a new method of analysis. Zoological Journal of the Linnean Society 130:449–467.

Williston, S. W. 1910. *Cacops, Desmospondylus*: new genera of Permian vertebrates. Bulletin of the Geological Society of America 21:249–284.

Zittel, K. A. von. 1888. Amphibia; pp. 337–437 in Handbuch der Paläontologie. I Abteilung. Palaeozoologie. Oldenbourg, Munich.

APPENDIX 1

Revised characters of Holmes (2013) and character scoring for IGCAGS V365 IVPP V 23862, and all available specimens for the modified character list.

(49) Subnarial lacrimal process: long (0); short (1); absent (2). [state 2 is added here for dissorophoids]

(53) Suborbital bar height: less than orbital height (0); subequal to orbital height (1); greater than half of the skull height (2).

(59) Osteoderm width: medium (0); wide, reaching at least the width of the two postparietals (1); narrow, not exceeding the maximum width of the transverse processes (2).

(67) Interclavicle: rhomboidal (0); quadrangular to pentagonal (1); bears a posterior stylus (2).

IGCAGS V365
???1???1????????????????????01????1?????00???0???2????-?????????????0????

IVPP V 23862
101?1?01?1100?10101111???01???0?0?01010???00?2?1?11?2-?1?11?1?0?000????0

*Anakamacops petrolicus*
10111?01?1100?10101111???01?1?0?010101000?1002?1211?2-?1?11?1?0?0000???0